EBAG9 could be a therapeutic target for various tumors constitutively expressing the molecule.

In summary, we demonstrate that EBAG9 is a tumor-promoting factor in both murine Renca RCC and human RCC. We propose that EBAG9 immunoreactivity is a new potential biomarker for prognosis of RCC and a treatment modality targeting EBAG9 will provide a novel therapeutic option for advanced RCC.

ACKNOWLEDGEMENTS

We thank T. Suzuki for her technical assistance.

REFERENCES

1. Watanabe T, Inoue S, Hiroi H, Orimo A, Kawashima H, Muramatsu M. Isolation of estrogen-responsive genes with a CpG island library. Mol Cell Biol 1998;18:442-9.
2. Tsuchiya F, Ikeda K, Tsutsumi O, et al. Molecular cloning and characterization of mouse EBAG9, homolog of a human cancer associated surface antigen: expression and regulation by estrogen. Biochem Biophys Res Commun 2001;284:2-10.
3. Suzuki T, Inoue S, Kawabata W, et al. EBAG9/RCAS1 in human breast carcinoma: a possible factor in endocrine-immune interactions. Br J Cancer 2001;85:1731-7.
4. Akahira JI, Aoki M, Suzuki T, et al. Expression of EBAG9/RCAS1 is associated with advanced disease in human epithelial ovarian cancer. Br J Cancer 2004;90:2197-202.
5. Takahashi S, Urano T, Tsuchiya F, et al. EBAG9/RCAS1 expression and its prognostic significance in prostatic cancer. Int J Cancer 2003;106:310-5.
6. Aoki T, Inoue S, Imamura H, et al. EBAG9/RCAS1 expression in hepatocellular carcinoma: correlation with tumour dedifferentiation and proliferation. Eur J Cancer 2003;39:1552-61.
7. Landis SH, Murray T, Bolden S, Wingo PA. Cancer statistics, 1999. CA Cancer J Clin 1999;49:8-31.
8. Moch H, Gasser T, Amin MB, Torhorst J, Sauter G, Mihatsch MJ. Prognostic utility of the recently recommended histologic classification and revised TNM staging system of renal cell carcinoma: a Swiss experience with 588 tumors. Cancer 2000;89:604-14.
9. Takeuchi T, Ueki T, Sasaki Y, et al. Th2-like response and antitumor effect of anti-interleukin-4 mAb in mice bearing renal cell carcinoma. Cancer Immunol Immunother 1997;43:375-81.
10. Nishimatsu H, Takeuchi T, Ueki T, et al. CD95 ligand expression enhances growth of murine renal cell carcinoma in vivo. Cancer Immunol Immunother 1999;48:56-61.
11. Gelb AB. Renal cell carcinoma: current prognostic factors. Union Internationale Contre le Cancer (UICC) and the American Joint Committee on Cancer (AJCC). Cancer 1997;80:981-6.
12. Dawson M. Initiation and maintenance of cultures. In: Bulter M, Dawson M editors. Cell culture labfax. Oxford: BIOS Scientific; 1992. p. 25-42.
13. Miyamoto T, Min W, Lillehoj HS. Lymphocyte proliferation response during Eimeria tenella infection assessed by a new, reliable, nonradioactive colorimetric assay. Avian Dis 2002;46:10-6.
14. Schumacher K, Haensch W, Roefzaad C, Schlag PM. Prognostic significance of activated CD8(+) T cell infiltrations within esophageal carcinomas. Cancer Res 2001;61:3932-6.
15. Shankaran V, Ikeda H, Bruce AT, et al. IFNgamma and lymphocytes prevent primary tumour development and shape tumour immunogenicity. Nature 2001;410:1107-11.
16. Pawelec G. Immunotherapy and immunoselection -- tumour escape as the final hurdle. FEBS Lett 2004;567:63-6.
17. Springer GF. Immunoreactive T and Tn epitopes in cancer diagnosis, prognosis, and immunotherapy. J Mol Med 1997;75:594-602.

18. Hakomori S. Glycosylation defining cancer malignancy: new wine in an old bottle. Proc Natl Acad Sci U S A 2002;99:10231-3.
19. Kudo D, Rayman P, Horton C, et al. Gangliosides expressed by the renal cell carcinoma cell line SK-RC-45 are involved in tumor-induced apoptosis of T cells. Cancer Res 2003;63:1676-83.
20. Thornton MV, Kudo D, Rayman P, et al. Degradation of NF-kappa B in T cells by gangliosides expressed on renal cell carcinomas. J Immunol 2004;172:3480-90.
21. Ritter G,Livingston PO. Ganglioside antigens expressed by human cancer cells. Semin Cancer Biol 1991;2:401-9.
22. Ito A, Levery SB, Saito S, Satoh M, Hakomori S. A novel ganglioside isolated from renal cell carcinoma. J Biol Chem 2001;276:16695-703.
23. Caldwell S, Heitger A, Shen W, Liu Y, Taylor B, Ladisch S. Mechanisms of ganglioside inhibition of APC function. J Immunol 2003;171:1676-83.
24. Manfredi MG, Lim S, Claffey KP, Seyfried TN. Gangliosides influence angiogenesis in an experimental mouse brain tumor. Cancer Res 1999;59:5392-7.
25. Engelsberg A, Hermosilla R, Karsten U, Schulein R, Dorken B, Rehm A. The Golgi protein RCAS1 controls cell surface expression of tumor-associated O-linked glycan antigens. J Biol Chem 2003;278:22998-3007.
26. Nakashima M, Sonoda K, Watanabe T. Inhibition of cell growth and induction of apoptotic cell death by the human tumor-associated antigen RCAS1. Nat Med 1999;5:938-42.
27. Gnarra JR, Zhou S, Merrill MJ, et al. Post-transcriptional regulation of vascular endothelial growth factor mRNA by the product of the VHL tumor suppressor gene. Proc Natl Acad Sci U S A 1996;93:10589-94.
28. Turner KJ, Moore JW, Jones A, et al. Expression of hypoxia-inducible factors in human renal cancer: relationship to angiogenesis and to the von Hippel-Lindau gene mutation. Cancer Res 2002;62:2957-61.
29. Ohm JE, Gabrilovich DI, Sempowski GD, et al. VEGF inhibits T-cell development and may contribute to tumor-induced immune suppression. Blood 2003;101:4878-86.
30. Sonoda K, Nakashima M, Kaku T, Kamura T, Nakano H, Watanabe T. A novel tumor-associated antigen expressed in human uterine and ovarian carcinomas. Cancer 1996;77:1501-9.

FIGURE LEGENDS

Fig. 1. Expression of EBAG9 siRNA suppresses tumor growth derived from murine renal cell carcinoma Renca cells in BALB/c mice. Subcutaneous primary Renca tumors were established by midflank injections of 10,000 tumor cells and intratumoral injections of either control scrambled siRNA or EBAG9 siRNA duplexes together with a transfection reagent GeneSilencer were performed twice a week in five mice per group when the initial tumor volumes reached 300 mm^3. Mice were sacrificed after 4-weeks siRNA administration and tumors were homogenized for protein extraction. *A*, Western blot analysis of lysates from *in vitro* culture Renca cells and tumor samples expressing either control scrambled siRNA or EBAG9 siRNA. *B*, Representative mice after 4-weeks siRNA treatment. Upper panel, mouse treated with control scrambled siRNA; Lower panel, mouse treated with EBAG9 siRNA. *C*, Tumor volume in EBAG9 siRNA-treated mice (n = 5) is reduced compared with control mice (n = 5). $^{*}P < 0.05$ at 4 weeks (EBAG9 siRNA *versus* scrambled siRNA).

Fig. 2. Overexpression of EBAG9 in Renca cells does not accerelate culture cell growth. *A*, RT-PCR analysis and Western blot analysis of Renca cells stably expressing human EBAG9 (Renca-EBAG9) or empty vector (Renca-vector). Upper panel, human EBAG9 mRNA is expressed in clones 3 and 4 of Renca-EBAG9 cells. Empty pcDNA3 vector was used as a negative control and pcDNA3 including EBAG9 cDNA as a positive control. Lower panel, EBAG9 protein is overexpressed in Renca-EBAG9 clones compared with Renca-vector clones or parental Renca cells. *B*, Doubling time of culture Renca cells. The numbers of cells in the exponential growth were counted every two days and doubling time was calculated according to a formula as described in Materials and Methods (n = 5 for each). *C*, Proliferative assay using WST-8 tetrasolium salt. Cells seeded into 96-well plates were transfected with control scrambled siRNA or EBAG9 siRNA duplexes (100 ng/well) and cell proliferation was evaluated on days 0, 2, and 4 (n = 3 for each). Absorbance at 450 nm (for formazan dye) was measured with absorbance at 620 nm for reference.

Fig. 3. Renca cells stably expressing EBAG9 develops large tumors in BALB/c mice. *A*, Representative mice 4 weeks after the inoculation of tumor cells. *B*, Volumes of tumors derived from Renca-EBAG9 cells are significantly larger compared with Renca-vector cells in BALB/c mice. Subcutaneous primary tumors were established by midflank injections of 10,000 tumor cells. $^{**}P < 0.01$ at 4 weeks (Renca-EBAG9 *versus* Renca-vector). Renca-vector #1, n = 16; Renca-vector #2, n = 6; Renca-EBAG9 #3, n = 6; Renca-EBAG9 #4, n = 8. *C*, Poorer prognosis of mice inoculated with Renca-EBAG9 cells compared with mice with Renca-vector cells. Disease-specific survival on day 100: $P = 0.0412$ (Renca-EBAG9 *versus* Renca-vector). Renca-vector #1, n =9; Renca-vector #2, n = 8; Renca-EBAG9 #3, n = 8; Renca-EBAG9 #4, n = 10.

Fig. 4. EBAG9 overexpression promotes renal subcapsular tumor growth by Renca cells in wild-type BALB/c mice. *A*, Representative tumors 25 days after the inoculation of tumor cells (10,000 cells). *B*, Volumes of Renca-EBAG9 tumors are larger than Renca-vector tumors in

BALB/c mice, whereas no significant difference of tumor volumes between Renca-vector and Renca-EBAG9 in BALB/c nude mice. $^{**}P < 0.0001$ on day 25 (Renca-EBAG9 *versus* Renca-vector). Renca-vector #1, n = 12; Renca-vector #2, n = 11; Renca-EBAG9 #3, n = 9; Renca-EBAG9 #4, n = 9. *C*, Lysis of Renca-EBAG9 and Renca-vector cells by tumor-specific cytotoxic T lymphocytes (CTLs). Splenocytes from Renca-bearing mice were cultured with Renca cells at a ratio of 20:1 pulsed with interleuikin-2 (1,000 U/ml) for 5 days. Lactate dehydrogenase release from cells with a damaged membrane was examined using CytoTox-ONE Reagent and fluorescence was measured with an excitation wave length of 560 nm and an emission wave length of 590 nm. *D*, Numbers of tumor infiltrating-lymphocytes positive for CD3, CD4, or CD8 immunostaining were microscopically examined in the high power field (HPF) of view at a magnification of 400X. BALB/c mouse spleen specimen was used as a positive control. $^{*}P < 0.05$ (Renca-EBAG9 *versus* Renca-vector).

Fig. 5. EBAG9 immunostaining in human kidney and renal cell carcinoma specimens. *A*, Normal kidney (IR score 0). EBAG9 is weakly expressed in the mesangial cells (arrow heads). *B*, Clear cell carcinoma (IR score 1+). EBAG9 is immunostained predominantly on the cell membrane in carcinous regions. *C*, Spindle cell carcinoma (IR score 3+). Intense immunostaining of EBAG9 is observed in the cytoplasm of sarcomatoid carcinous regions. *D*, Lung metastatic tumors (IR score 3+). Intense immunoreactivity of EBAG9 is observed in metastatic tumors with high IR scores. Bars represent 50 μm.

Fig. 6. Association of immunocytochemical staining for EBAG9 with disease-specific survival of 78 RCC patients. Five-year disease-specific survival of the patients with high EBAG9 immunoreactivity (IR score 3+, n = 19) was significantly worse than the patients with IR scores 0-2+ (n = 59) (55% *versus* 91%, $P = 0.0007$, by log-rank test).

Supplementary Table 1 *Association between EBAG9 immunoreactivity and clinicopathological parameters in human RCC patients*

Variable	n	EBAG9 immunoreactivity		*P* Value[a]
		Negative	Positive[b]	
Patients	78	10	68	
Lymph node status				> 0.9999
Positive	6	0	6	
Negative	72	10	62	
Metastatic status				0.5857
Positive	7	0	7	
Negative	71	10	61	
Age		57.5 ± 8.1[c]	54.1 ± 11.7	0.3849
Sex				0.3735
Male	64	7	57	
Female	14	3	11	
Infiltration				0.3263
α	43	7	36	
β, γ	35	3	32	
Grade				0.0606
1	24	6	18	
2, 3	54	4	50	
Histological type				0.0126*
Clear cell	51	10	41	
Others	27	0	27	
Vascular infiltration				0.0109*
Positive	29	0	29	
Negative	49	10	39	
Pathological stage				0.0017*
T1	43	10	33	
≥T2	35	0	35	

[a]Evaluated by the student-t test/ Fisher's exact probability test.

[b]Defined positive if >5% of cells were stained.

[c]Mean ± standard deviation.

*$P < 0.05$.

Supplementary Table 2 *Correlation between 5-year cancer-specific survival and clinicopathological parameters in RCC patients*

Variable	n	Survival (%)	*P* Value[a]
Patients	78		
Age			0.5828
<60	49	85.5	
≥60	29	77.4	
Grade			0.0254*
1	24	95.7	
2, 3	54	76.8	
Histological type			0.0205*
Clear cell	51	89.8	
Others	27	70.4	
EBAG9 immunoreactivity			0.0007*
Low (0, 1+ & 2+)	59	91.2	
High (3+)	19	55	
Vascular infiltration			0.0003*
Positive	29	62.4	
Negative	49	93.9	
Lymph node status			0.0002*
Positive	6	33.3	
Negative	72	86.9	
Infiltration			< 0.0001*
α	41	97.5	
β, γ	37	65.5	
Pathological stage			< 0.0001*
T1	43	97.6	
≥T2	35	63.6	
Metastatic status			< 0.0001*
Positive	7	0	
Negative	71	91.2	

[a]Determined by the log-rank test.

*$P < 0.05$.

Supplementary Table 3 *Multivariate anlalysis of prognostic factors in Cox regression hazard model*

Variable	Relative risk	95% confidence interval	*P* value
Grade (2, 3/ 1)	1.081	0.099 - 11.835	0.9490
Vascular infilatration (positive/ negative)	0.938	0.213 - 4.139	0.9326
Pathological stage (≥T2/ T1)	8.702	0.973 - 77.831	0.5290
Lymph node status (positive/ negative)	0.385	0.087 - 1.700	0.2077
Infiltration (β, γ/ α)	4.342	0.485 - 38.883	0.1892
Histological type (others/ clear cell)	3.874	0.817 - 18.365	0.0880
EBAG9 immunoreativity (3+/ 0,1+, and 2+)	5.092	1.010 - 25.662	0.0485*
Metastatic status (positive/ negative)	42.534	7.138 - 253.469	< 0.001*

*$P < 0.05$

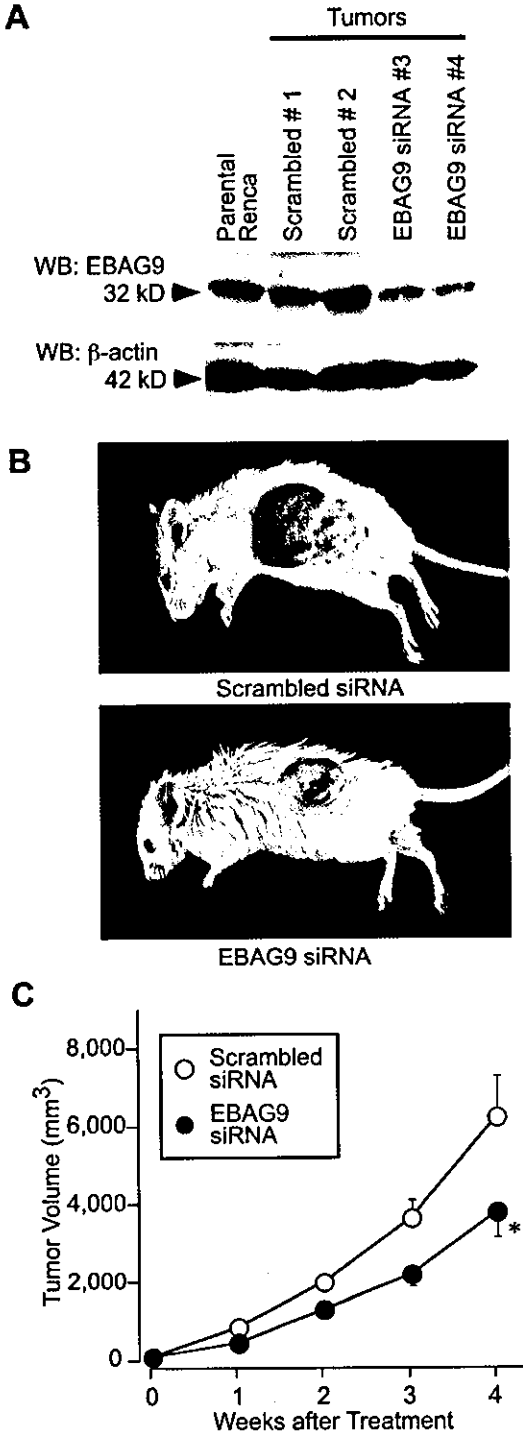
A
Tumors
Parental Renca
Scrambled # 1
Scrambled # 2
EBAG9 siRNA #3
EBAG9 siRNA #4
WB: EBAG9
32 kD
WB: β-actin
42 kD
B
Scrambled siRNA
EBAG9 siRNA
C
Tumor Volume (mm3)
8,000
6,000
4,000
2,000
0
Scrambled siRNA
EBAG9 siRNA
*
0
1
2
3
4
Weeks after Treatment

Fig. 1

A

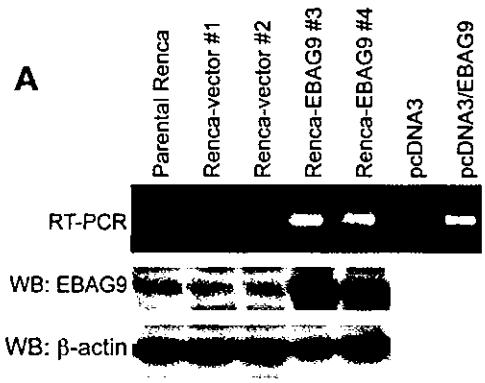

B

	Doubling Time (h)
Renca-vector #1	25.4 ± 1.1
Renca-vector #2	27.5 ± 0.6
Renca-EBAG9 #3	23.2 ± 1.2
Renca-EBAG9 #4	24.6 ± 1.2

C

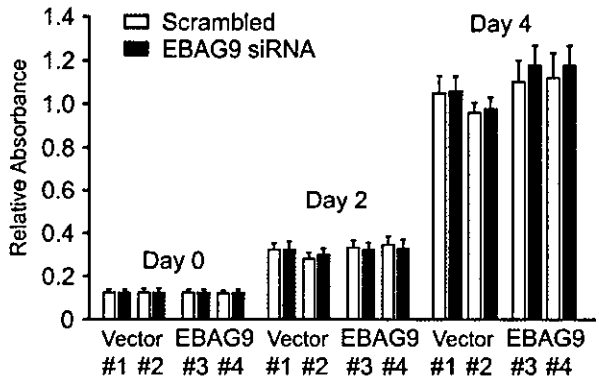

Fig. 2

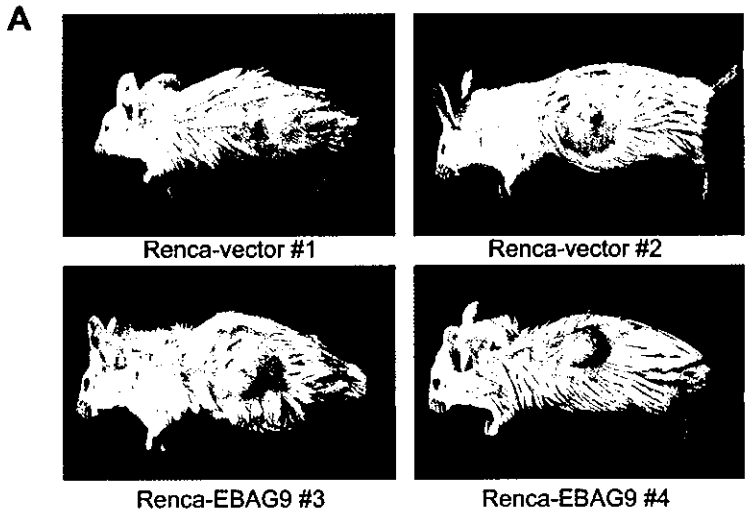
A
Renca-vector #1
Renca-vector #2
Renca-EBAG9 #3
Renca-EBAG9 #4

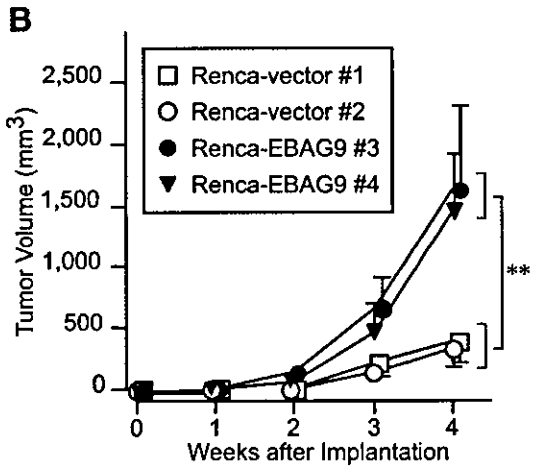
B
Renca-vector #1
Renca-vector #2
Renca-EBAG9 #3
Renca-EBAG9 #4
Tumor Volume (mm3)
2,500
2,000
1,500
1,000
500
0
0
1
2
3
4
Weeks after Implantation
**

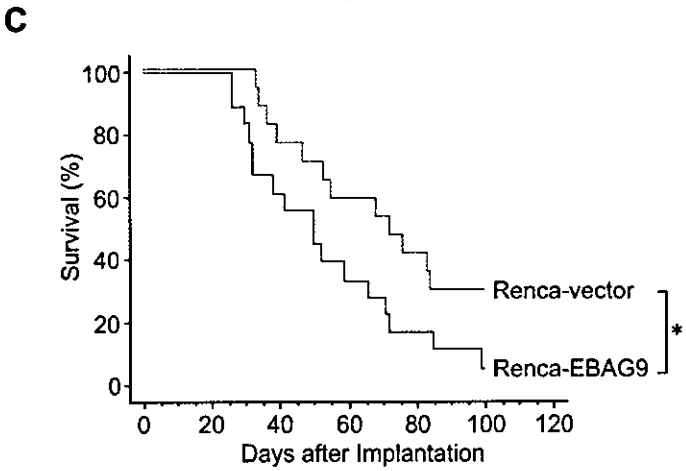
C
Survival (%)
100
80
60
40
20
0
0
20
40
60
80
100
120
Days after Implantation
Renca-vector
Renca-EBAG9
*

Fig. 3

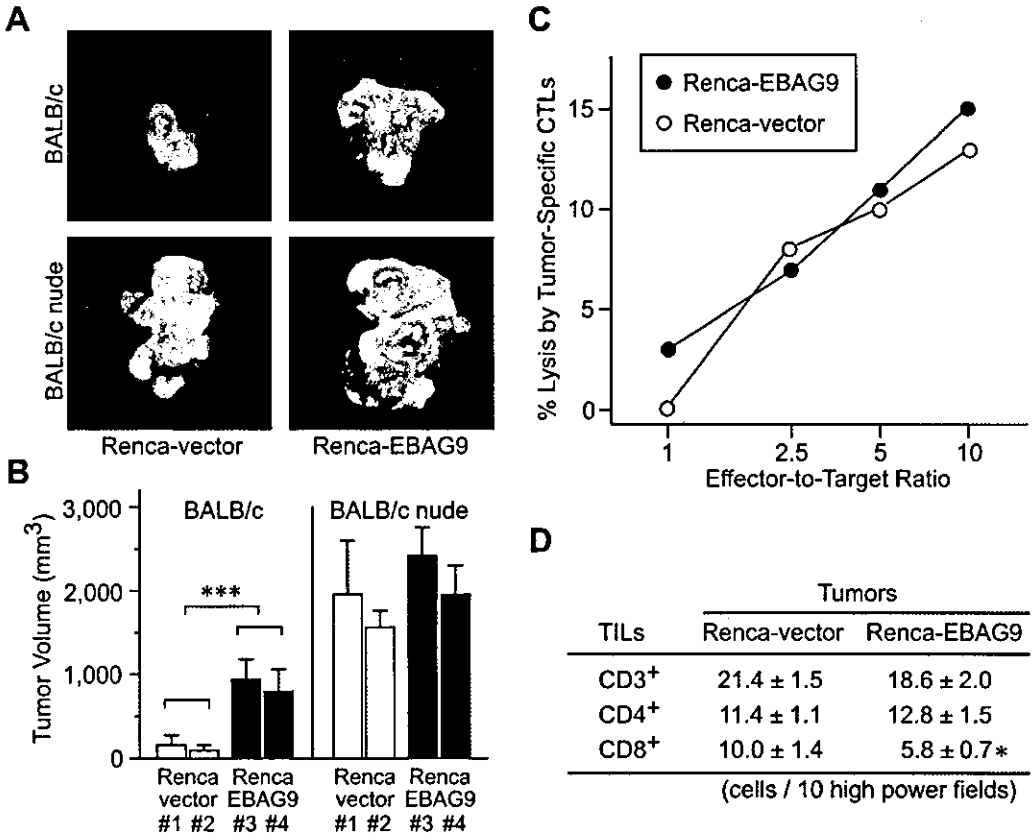

D

TILs	Tumors	
	Renca-vector	Renca-EBAG9
$CD3^+$	21.4 ± 1.5	18.6 ± 2.0
$CD4^+$	11.4 ± 1.1	12.8 ± 1.5
$CD8^+$	10.0 ± 1.4	5.8 ± 0.7*

(cells / 10 high power fields)

Fig. 4

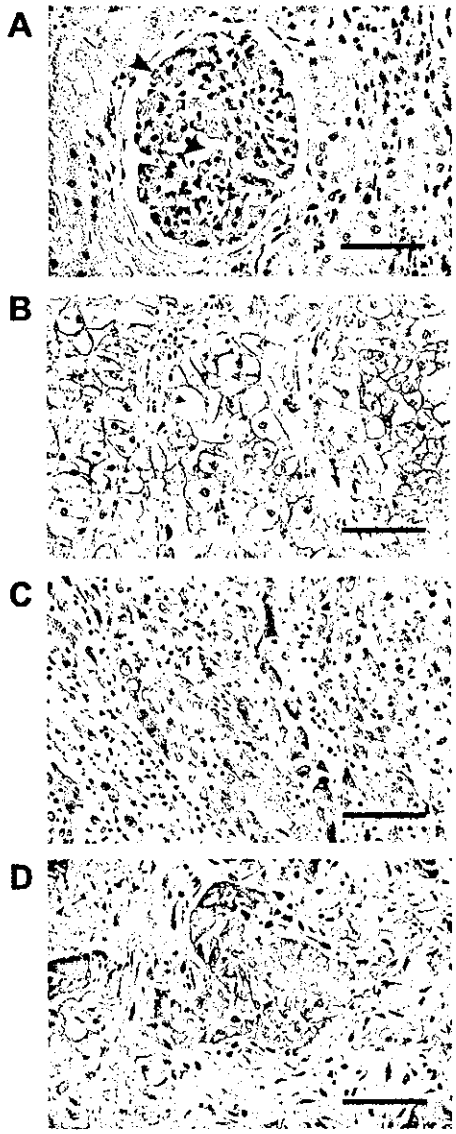

Fig. 5

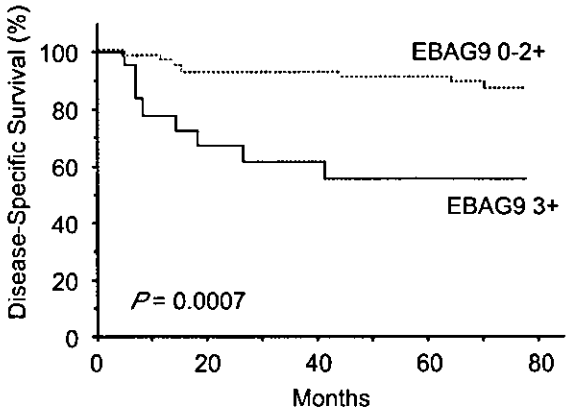
Disease-Specific Survival (%)
100
80
60
40
20
0
EBAG9 0-2+
EBAG9 3+
P= 0.0007
0
20
40
60
80
Months

Fig. 6

CHAPTER 16

RING Finger-B Box-Coiled Coil (RBCC) Proteins as Ubiquitin Ligase in the Control of Protein Degradation and Gene Regulation

Kazuhiro Ikeda, Satoshi Inoue, Masami Muramatsu

Abstract

The protein family harboring the RING finger motif, de fined as a linear array of conserved cysteines and histidines, has grown enormously in the last decade. The members of the family are involved in various biological processes including growth, differentiation, apoptosis, transcription and also in diseases and oncogenesis. It has been postulated that the RING finger domains have crucial roles in these phenomena themselves, in some cases, working with other domains in other proteins, although the precise mechanisms and common features of RING finger function have not been fully elucidated. However, most recently, an accumulating body of evidence has revealed that some of the RING finger proteins work as E3 ubiquitin ligases in ubiquitin-mediated specific protein degradation pathway. In this review, we focus on the RING finger protein with special reference to E3 ligase.

Structure of RING Finger

The RING finger protein sequence motif was first identified in the human gene RING1 – Really Interesting New Gene 1 – which is located proximal to the major histocompatibility region on chromosome 6.[1,2] The RING finger motif can be defined as a unique linear series of conserved cysteine and histidine residues: Cys-X_2-Cys-X_{11-16}-Cys-X-His-X_2-Cys-X_2-Cys-X_{7-74}-Cys-X_2-Cys (RING-CH or C_3HC_4 type), where X can be any amino acid (Fig. 1). So far, three-dimensional structures of RING domains from human PML (for promyelocytic leukemia protein),[3] immediate early equine herpes virus (IEEHV) protein,[4] human recombination-activating gene 1 protein (RAG1),[5] human MAT1 (for menage a trois-1 protein)[6] and human Cbl (for Casitas B-lineage lymphoma protein)[7] with a cognate ubiquitin-conjugating enzyme (E2) have been solved at atomic resolution. These studies have confirmed that the RING finger binds zinc ions in a similar manner as the classical zinc finger motif. Particularly, the RING finger is composed of a unique 'cross-brace' arrangement with two zinc ions and folds into a compact domain comprising a small central β sheet and an α helix. There are subfamilies of RING fingers which have Cys5 substituted with histidine (RING-H2) and a cysteine or histidine substituted with other metal binding residues such as aspartic acid and threonine.[8,9] Although the RING domain was initially found

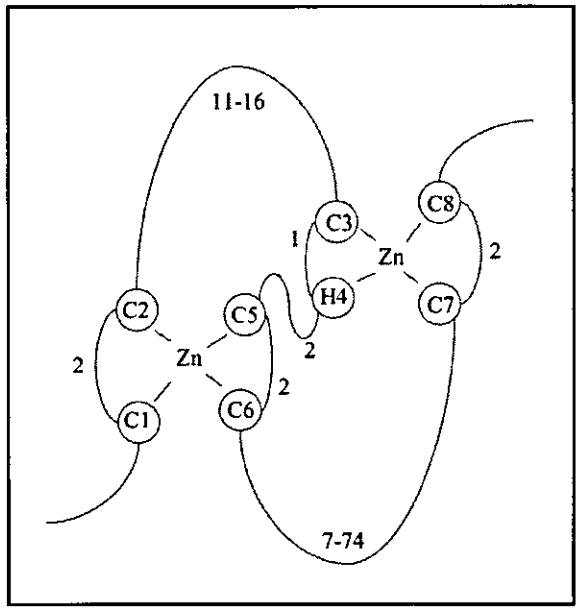

Figure 1. Schematic representation of the structure of RING finger domain. The metal-ligand residues, either cysteine (C) or histidine (H), are shown as numbered spheres. The numbers next to the loops connecting the metal-ligand residues indicate the minimum and maximum number of loop residues.

in only a few genes, more than 3000 proteins harboring the RING finger domain have been detected from diverse eukaryotes in the SMART database as of July 2003. Because of this evolutional conservation and variation in loop lengths, the RING domain appears to have a considerable flexibility within the rigid structure.

Family of RING Finger Protein

The RING fingers and their variants are generally located close to an amino or carboxyl terminus though there are no fixed rules. Most of the RING finger is associated with certain protein domains to form larger conserved motifs which may define the func-

Zinc Finger Proteins: From Atomic Contact to Cellular Function, edited by Shiro Iuchi and Natalie Kuldell.

tion of the protein, thus the family being divided into subfamilies along with the associated domains (Fig. 2). A similar domain architecture often corresponds with a similar function. For instance, TRAFs (for tumor necrosis factor (TNF) receptor-associated factors) 2-5 have an N-terminal RING domain followed by five zinc fingers, a coiled coil, and a C-terminal TRAF domain.[10] TRAF1 has all of these domains except for the RING. Members of TRAF family have been shown to be involved in TNF-related cytokine signal transduction through interactions between their TRAF domains and the intracytoplasmic parts of receptors of the TNF receptor family which are suicide receptors to transfer apoptotic signals into the cells.[11-13]

The inhibitors of apoptosis gene family, IAP1, IAP2 and XIAP, have a RING domain at their C termini and BIR (baculovirus IAP repeat) domain at their N termini. The BIR domains of the proteins bind and inhibit caspase.[14,15] Interestingly, the RING fingers of XIAP and IAP2 possess E3 ubiquitin ligase activity and are thought to be responsible for self-degradation when an apoptotic signal is transduced.[16] In addition, the anti-apoptotic activity of the protein is lost when the RING domain is mutated.[17]

There are interesting subfamilies uniquely possessing two RING fingers. Triad1 (for two RING fingers and DRIL1) and parkin have two RING finger domains separated by the double RING finger linked (DRIL) domain. Triad1 was identified as a nuclear RING finger protein, which is up-regulated during retinoic acid induced granulocytic differentiation of acute leukemia cells.[18] Parkin is a responsible gene for familial autosomal recessive Parkinson's disease.[19,20] Parkin binds to the E2 ubiquitin-conjugating enzymes through its C-terminal RING finger and has ubiquitin–protein ligase activity.[21] Parkin ubiquitinates and promotes the degradation of a putative G protein-coupled transmembrane polypeptide, Pael (parkin-associated endothelial-like) receptor, the insoluble form of which is accumulated in the brains of Parkinson's disease.[22] The insoluble parkin overexpressed in cells causes unfolded protein-induced cell death, whereas coexpression of Parkin suppresses the accumulation of Pael receptor and subsequent cell death.[21] Parkin also ubiquitinates and promotes the degradation of CDCrel-1 (for cell division cycle related-1) and itself.[23] Familial-linked mutations disrupt the ubiquitin–protein ligase function of Parkin and impair Parkin and CDCrel-1 degradation.

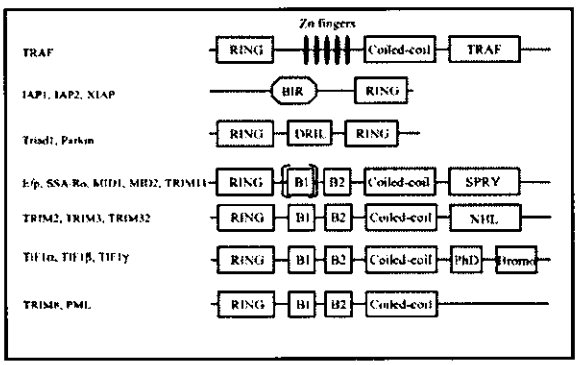

Figure 2. Structures of the RING finger protein family. Representative RING finger proteins with frequently associated domains are presented.

Function of RING Finger

It has been shown in early studies that the RING finger proteins have crucial roles in the growth, differentiation, transcription, signal transduction and oncogenesis.[24] For example, PML is fused to the retinoic acid receptor α (RARα) in acute promyelocytic leukemia (APL) translocation,[25-27] BRCA1 is mutated in early-onset breast cancer and ovarian cancer,[28] TIF1α is a positive cofactor of nuclear hormone receptors[29] and TRAF transduces signals from members of the TNF receptor superfamily to the transcription factor NF-κB.[14] Although those studies appear to show some essential roles played by the RING finger domains in the function of these proteins, the general function of the RING finger domain has not been resolved. However, recently, it was uncovered that the RING finger proteins are involved in the ubiquitin-mediated protein degradation pathway.

The ubiquitin-dependent protein degradation is a specific and sophisticated mechanism in which a target protein to be destroyed is tagged with the ubiquitin. Ubiquitination is accomplished by a complex process involving ubiquitin-activating enzyme (E1), ubiquitin-conjugating enzyme (E2) and ubiquitin ligase (E3).[30] Ubiquitin ligase mediates the transfer of ubiquitin from E2 to a substrate, marking it for degradation by the 26S proteosome. Therefore, E3 enzyme is thought to be important for the specific recognition of the substrate in the ubiquitination pathway. There is accumulating evidence that RING finger domains are identified in E3 complexes and proteins, suggesting the broad use of these domains for ubiquitination. As mentioned above, RING finger domain has the conserved cysteine and histidine residues. The C_3HC_4 type RING finger is found in several E3 proteins including Cbl,[31] BRCA1,[32] Efp (for estrogen-responsive finger protein)[33] and Mdm2 (for murine double minute 2).[34] The RING-H2 subtype is found in Rbx1 (for RING box protein 1) and Apc11 (for anaphase promoting complex (APC) subunit 11) in SCF (Skp1-Cullin-F-box) and APC E3 complexes,[35] respectively, and other ubiquitin ligases. Thus, evidence is accumulating that the RING finger proteins has crucial roles as an E3 ubiquitin ligase in diverse biological functions and diseases. Cbl is one of the initially identified E3 ligase which is involved in the regulation of various tyrosine kinase-linked receptors such as growth factor receptors (for example EGF and PDGF receptors), cytokine receptors and immuno-receptors (for example T-cell, B-cell and Fc-receptors).[36] Cbl recognizes activated protein tyrosine kinases and recruits E2 ubiquitin conjugating enzymes through its SH2 and RING finger domain, respectively. For EGF and PDGF receptors, increased recruitment of Cbl to the activated receptor complex leads to enhanced ubiquitination and degradation of the activated receptor. In contrast, oncogenic mutation in the Cbl RING finger which fails to bind E2 ubiquitin conjugating enzymes abrogates Cbl-mediated EGF receptor ubiquitination and degradation.[37] Thus, it appears that Cbl functions as an adapter to recruit the ubiquitination machinery to activated tyrosine kinase-linked receptors and stimulates receptor ubiquitination and degradation. This causes enhanced down-regulation of the receptor from the cell surface and attenuation of growth factor receptor signaling.

The RING finger protein Mdm2 is identified as an E3 ubiquitin ligase of the tumor-suppressor protein p53 which is a transcription factor and a potent inhibitor of the cell cycle. Mdm2 can bind to p53 and promote its ubiquitination and subsequent degradation by the proteasome.[38,39] It is also known that Mdm2 can ubiquitinate itself, suggesting that some of E3s self-regulate their own stability. The RING finger of Mdm2 is necessary for

both p53 ubiquitin and Mdm2 auto-ubiquitination. Substitution of the Mdm2 RING finger domain with the RING finger from another RING protein maintains the autoubiquination and degradation of Mdm2 but is not able to stimulate p53 ubiquitination. Moreover, mutations in the RING finger domain do not impair binding capacity between Mdm2 and p53. These observations suggest that the RING finger domain appears to be required for specific recognition of substrates in some degree, but is not generally involved in substrate binding.[40]

RBCC/TRIM Subfamily

Frequently, the RING is associated with cysteine-rich B-box domains followed by a predicted coiled coil domain. The B-box domain can be defined as a series of conserved cystein and histidine residues: B1 [Cys-X_2-Cys-X_{7-10}-Cys-X_2-Cys-X_{4-5}-Cys-X_2-Cys/His-X_{3-6}-His-X_{2-8}-His] and B2 [Cys-X_{2-4}-His/Cys-X_{4-9}-Cys-X_2-Cys/His-X_4-Cys/His-X_2-His/Cys] where X can be any amino acid. Structural analysis revealed that it consists of 15 or fewer β-strands.[41] The coiled coil is a common protein motif involving a number of α-helices wound around each other in a highly organized manner and is often used to control oligomerization.[42] These RING, one or two B-boxes and a coiled coil domain motifs are called RBCC or tripartite motif (TRIM)(Fig. 3).[43] This largest subfamily was first identified in a putative transcriptional regulator, Xenopus XNF7[24] and about 50 members have been identified since then. Though either one or two B-boxes are present, the spacing between the RING, B-boxes and the coiled coil is highly conserved with 38-40 residues between the RING and first B-box, and less than 10 amino acids between the second B-box and the coiled coil. There is no apparent homology among these separating sequences. According to the recent progress of genomic analysis, it was revealed that the chromosomal localization of the RBCC/TRIM subfamily genes has an intriguing feature. Although the genes encoding the RBCC/TRIM family members are dispersed throughout the genome, there are two distinct clusters on chromosomes 11p15 and 6p21-22 (Fig. 4). *TRIM22, SSA1/TRIM21, TRIM34, TRIM6, TRIM5, TRIM3* and *SS-56* are clustered in 11p15. *RFP/TRIM27, TRIM31, TRIM10, TRIM15, TRIM26, TRIM38, TRIM39, TRIM40* and *HZFW1* are clustered in 6p21-22. In particular, mRNAs for *TRIM 21, 22* and *34* are shown to be up-regulated by interferons.[44-46] These findings suggest that duplication of an ancestral *RBCC/TRIM* gene at these genomic loci may have occurred and, regulation and function may be conserved to some extents in these genes.[43]

The RBCC/TRIM proteins are associated with certain domains such as B30.2-like or SPRY, NHL, PHD and BROMO domains at their C-terminus. These additional domains may contribute to the function of the subfamily. The B30.2-like domain is a series of 160-170 amino acids containing three highly conserved motifs (LDP, WEVE and LDYE) which is named after the B30-2 exon within the human class I histocompatibility complex locus. The SPRY domain, which was originally named from SPla and the RYanodine Receptor, is composed of around 140 amino acids containing the latter two conserved motifs in B30.2-like domain. At present, the B30.2-like domain is considered as a subclass of the SPRY domain family. The SPRY domain is contained in many of the RBCC/TRIM subfamily including XNF-7, RPT-1, SSA-Ro and STAF50. The significantly conserved SPRY domains imply the biological importance of this gene, however the function of the SPRY domain is not known. The NHL domain name was derived from the three founding members: NCL-1, HT2A, and LIN-41.[47] NCL is involved in rRNA metabolism. HT2A was identified as an interacting partner of the

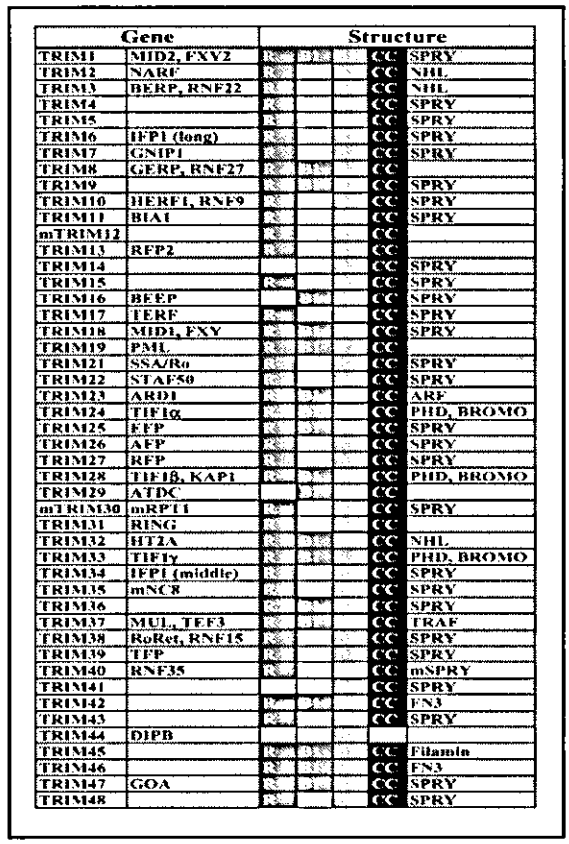

Figure 3. RBCC/TRIM family genes. The gene names are listed in numerical order of *TRIM* genes followed by commonly used names in the second column. Their domain structures are schematically shown to the right.

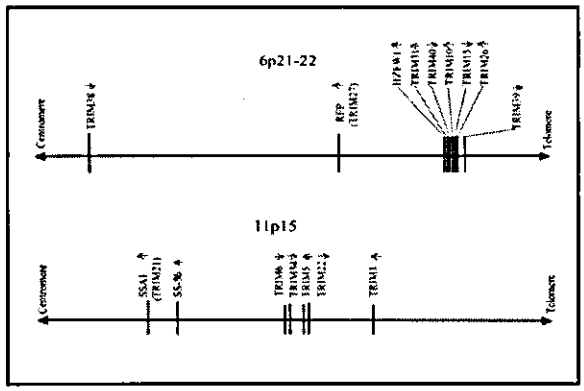

Figure 4. Clustered localization of the *RBCC/TRIM* genes in 6p21-22 and 11p15. *TRIM22, SSA1, TRIM34, TRIM6, TRIM5, TRIM3* and *SS-56* are clustered in 11p15, whereas *RFP, TRIM31, TRIM10, TRIM15, TRIM26, TRIM38, TRIM39, TRIM40* and *HZFW1* are clustered in 6p21-22. The sense strand orientations of each gene are indicated by the arrows.

HIV Tat protein and Lin41 is involved in posttranscriptional regulation of mRNA. The NHL motif has a slight homology with WD40 domain, suggesting a protein-protein interaction. The C-terminal PHD fingers and bromodomains are found in TIF1α and KAP1/TIF1β. The PHD domain is a motif characteristically defined by seven cysteines and a histidine that are highly homologous to the RING motif and is contained in some transcription factors. The PHD domain of MEKK1 (MEK kinase 1) exhibited E3 ubiquitin ligase activity toward ERK (extracellular signal-regulated protein kinase) 2, suggesting a negative regulatory mechanism for decreasing ERK1/2 activity.[48] The bromodomain is also found in transcription factors, can bind histones with acetylated lysines and appears to be involved in chromatin remodeling.[49] KAP1/TIF1β and TIF1α are involved in transcriptional regulation. Genes belonging to this RBCC/TRIM family are implicated in a variety of processes such as development and cell growth and are involved in several human diseases. PYRIN,[50] MID1 (Midline 1)[51] and MUL (for mulibrey nanism proteins)[52] are mutated in familial Mediterranean fever, X-linked Opitz/GBBB syndrome and mulibrey nanism, respectively, whereas PML, RFP (ret finger protein) and TIF1α acquire oncogenic activity when fused to RARα, RET or B-raf, respectively.

It has been shown that the RBCC/TRIM proteins can oligomerize through their coiled coil domains. In homodimerization of RFP proteins, the coiled coil region with the B-box but not the RING finger is required.[53] In this case, while the B-box is not an interacting interface itself, the mutation of conserved cysteine residues within the B-box affects the ability of RFP to multimerize, suggesting that its structural integrity is necessary for this interaction to occur.[53] The coiled coil domain of RFP is also necessary for interaction with Enhancer of polycomb protein (EPC) to repress gene transcription.[54] The homodimerization and binding with EPC occurs with the proximal coil in RFP protein. RFP also directly interacts and colocalizes with PML in a subset of the PML NBs (nuclear bodies).[55] This interaction is mediated by the RFP B-box and the distal two coils. The association of RFP with the PML NBs is altered by mutations that affect RFP/PML interaction and in APL patients-derived cells. These results indicate that RFP have an important role in regulating cellular growth and differentiation. MID1 protein, which is mutated in patients with Opitz GBBB syndrome, and the highly related gene MID2 also make both homo- and hetero-dimers mediated by the coiled coil motifs. The dimerization is a prerequisite for the association of MID and Alpha 4 (a regulatory subunit of PP2-type phosphatases) and the complex formation with microtubules which seems important for normal midline development.[56] In contrast, it has been shown that the entire RBCC/TRIM domain is required for hetero-oligomerization or binding natural ligands. The RBCC region of KAP1/TIF1β associates with the KRAB (Krüppel-associated box) transcriptional repressor domain of KOX-1.[57] From extensive studies of the interaction, it has been revealed that the interaction is specific for the KAP1 RBCC/TRIM domain. Namely, when each RBCC/TRIM motifs of KAP1 was swapped with other corresponding ones of MID1, KAP1 did not bind the KRAB domain any more. Therefore, each domain of the RBCC may function as an independent functional unit and have important roles in the specific recognition of interacting partners or oligomers formation. In other RBCC/TRIM proteins, only one copy of the B-box motif is present, but inspection of the whole family reveals a conserved residue spacing between the RING, B-box and coiled coil domains.[43] This strongly suggests that the overall architecture of the RBCC/TRIM motif is highly conserved, perhaps relating to the motif acting as a scaffold for higher-order protein-protein interactions.[57] Molecular modeling suggests that the position and orientation of the B-box (adjacent to the coiled coil) would be critical for the correct alignment of the α-helices that form the coiled coil. Interestingly, unlike the RING and coiled coil motifs, the B-box is only found in RBCC/TRIM family members suggesting that it is a critical determinant of the overall motif and its function.[43]

As mentioned above, the latest findings of RING fingers in E3 ubiquitin ligases imply that the members of this RBCC/TRIM subfamily are potential candidates for specific regulators/adopters in ubiquitin-dependent protein degradation. In fact, some genes belonging to the subfamily has been proven to act as E3 ligase. We next discuss such genes focusing on the recent findings.

Ring Fingers that Act As E3 Ligases

Efp

Estrogen-responsive finger protein (Efp) is a member of the RING-finger, B1 and B2-boxes, coiled coil and SPRY (RBCC-SPRY) subfamily in the RING finger family. Efp was isolated as an estrogen-responsive gene by genomic binding-site cloning using a recombinant estrogen receptor (ER) protein.[58] The estrogen-responsive element (ERE) to which ER can bind is found at the 3'-untranslated region (UTR) in the *Efp* gene and the gene's expression is predominantly detected in female reproductive organs including uterus, ovary and mammary gland[59] and in breast and ovarian cancers.[60] Estrogen-induced expression is found in the uterus, brain and mammary gland cells. *Efp* knockout mice have an underdeveloped uterus and estrogen responses of uterin cells from knockout mice are markedly attenuated, suggesting that Efp is necessary for estrogen-induced cell growth.[61] Moreover, tumor growth of breast cancer MCF7 cells implanted in female athymic mice has been demonstrated to be reduced by treatment with antisense Efp oligonucleotide. In contrast, Efp-overexpressing MCF7 cells in ovariectomized athymic mice generate tumors in the absence of estrogen.[33] These results indicate that Efp mediaes estrogen-dependent growth in breast cancer cells. We identified 14-3-3Σ which is responsible for reduced cell growth, as a binding factor to Efp and found an accumulation of 14-3-3Σ in *Efp* knockout mouse embryonic fibroblasts. Furthermore, it has been revealed that Efp is an ubiquitin ligase (E3) that targets proteolysis of 14-3-3Σ. Specifically, the RING which preferentially bound to ubiquitin-conjugating enzyme UbcH8 has been shown to be essential for the ubiquitination of 14-3-3Σ. Our findings provide an insight into the cell-cycle machinery and tumorigenesis of breast cancer by identifying 14-3-3Σ as a target for proteolysis by Efp, leading to cell proliferation. The degradation of 14-3-3Σ is subsequently followed by dissociation of the protein from cyclin–Cdk complexes, leading to cell cycle progression and tumor growth (Fig. 5).

MID1, MID2

Opitz GBBB syndrome (OS; Opitz syndrome) is a genetically and phenotypically complex disorder defined by characteristic facial anomalies, structural heart defects, as well as anal and genital anomalies.[62,63] A positional cloning approach has revealed a candidate gene designated *MID1*[51] which is a member of the RBCC-SPRY family. Most of the mutations identified so far in patients with Opitz syndrome cluster in the SPRY domain of

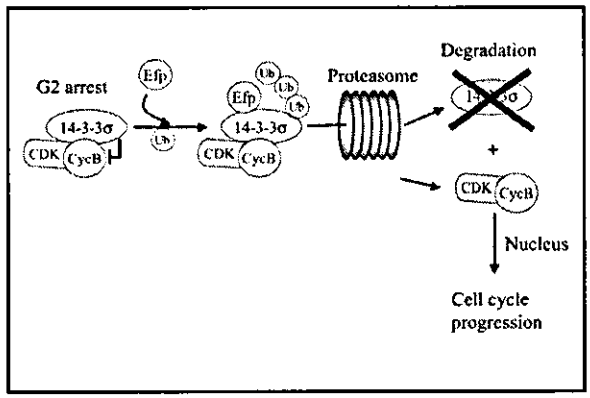

Figure 5. Models of Efp action as E3 ligase. Estrogen-induced RING finger protein Efp recognizes a cell cycle inhibitor 14-3-3Σ which keeps Cyclin B in cytoplasm. Efp modifies 14-3-3Σ with ubiquitin and the resulting ubiquitinated 14-3-3Σ is recruited to 26S proteosome to be destroyed. The dissociated cyclin B is now capable of entering the nucleus where it drives cell cycle.

MID1. It has been shown that MID1 associates with microtubules, whereas mutant forms of MID1 do not.[64] These results suggest that MID1 has a physiological role in microtubule dynamics.

Recently, the α4 protein, a regulatory subunit of protein phosphatase 2A (PP2A)[65] was isolated by yeast two-hybrid screening with MID1 as bait. It was demonstrated that the B-box 1 is sufficient for a strong interaction with α4. MID2,[66] which is highly similar to MID1, also binds α4. Cellular localizations of MID1 and α4 are coincident with cytoskeletal structures and MID1 with a mutation at the C terminus that mimics the mutant protein of some individuals with OS results in the formation of cytoplasmic clumps containing both proteins. The identified substrate for E3 ligase activity of MID1 is a cytosolic PP2A. In contrast, addition of a proteasome inhibitor to OS-derived fibroblasts expressing dysfunctional MID1 does not cause either enrichment of PP2A or accumulation of the enzyme's polyubiquitinated forms,[67] suggesting that MID1 mutations result in decreased proteolysis of the C subunit of PP2A in individuals with OS.

PML

PML also belongs to a subfamily of proteins containing a RBCC/TRIM motif.[43,68] PML has been implicated in the pathogenesis of acute promyelocytic leukemia that arises following a reciprocal chromosomal translocation that fuses the *PML* gene located on chromosome 15 with the retinoic acid receptor alpha (*RARα*) gene located on chromosome 17. The resulting PML-RARα fusion protein preserves most of the functional domains of both PML and RARα, but it lacks C-terminus of PML and N-terminus of RARα The fusion protein shows cell type- and promoter-specific differences from the wild type RARα,[25,26,69] while it maintains a responsiveness to retinoic acid. Overexpression of PML-RARα inhibits vitamin D3 and transforming growth factor β-induced differentiation and also reduces serum starvation-induced apoptosis in U937 cells.[70] In addition, dimerization of PML with PML-RARα is required to block differentiation.[71] Thus, PML-RARα is considered to function as a dominant negative protein by interfering with the function of PML and RARα.

In normal cells, cellular distribution of PML is found to form a discrete subnuclear compartment (nuclear body, NB)[72,73] or PML oncogenic domain.[74] Other proteins containing Sp100[75] and PLZF (for promyelocytic leukemia zinc finger)[76] have been reported to localize to the NBs. Interestingly, PLZF-RARα fusion protein is also found in a rare form of APL.[77] It is shown that the nuclear bodies were dispersed into a microspeckle pattern in APL cells but reformed with retinoic acid treatment by which APL cells differentiated into granulocytes. In addition, the NB is the preferred site where the early steps of transcription and replication of DNA virus occurs.[78] Therefore, the regulation of NB formation is thought to be involved in the pathogenesis of APL. Recently, PML is shown to be covalently modified by SUMO-1 (Small Ubiquitin-like Modifier-1) of ubiquitin-like proteins.[79] Mutations in the PML RING finger disrupt the nuclear body formation in vivo[3,69] and cause a failure of growth suppression,[80,81] apoptosis and anti-viral activities[82] of PML. The dependence on an intact RING finger for PML NBs formation implies specific protein interactions regulated by the RING structure. Recent studies have shown that PML RING interacting with the SUMO-1 E2 enzyme UBC9 is SUMO modified and the sumolylation of PML has an important role in regulating the formation of NBs.[83]

PML has two B-boxes (B1 and B2) adjacent to the RING domain. Mutations of conserved zinc-chelating residues in B1 and/or B2 boxes collapsed PML NB formation, whereas they did not affect PML oligomerization.[84] PML B-boxes are also involved in growth suppression.[80] It has been revealed that PML is sumoylated in B1 box which is responsible for binding of the 11S proteasomal subunit to PML NBs.[85]

The coiled coil region in PML is indispensable for multimerization or heterodimerization with PML-RARα,[69,71,86] formation of PML NB and growth suppression activity.[80] Notably, the important role of the coiled coil domain for the complex formation is also suggested from the studies of other RBCC/TRIM subfamily.[43,57]

TRIM8

TRIM8, a member of RBCC subfamily, is shown to interact with SOCS-1 (suppressor of cytokine signaling-1) which is induced by cytokines and inhibits cytokine signaling by binding to downstream signaling molecules such as JAK (Janus kinase) kinases.[87-89] The B-box coiled coil region of TRIM8 is sufficient for efficient interaction with SOCS-1, but the RING portion of the protein is not required for the binding. By contrast, both the SOCS box and the SH2 domain in SOCS-1 appear to be necessary for the interaction between SOCS-1 and TRIM8. It was found that exogenous coexpression of TRIM8/GERP with SOCS-1 decreased the stability of SOCS-1 protein and TRIM8 restored the IFN-γ-mediated transcription which was inhibited by the expression of SOCS-1.[90] These results suggest that TRIM8 is the putative E3 ligase for SOCS-1 and inhibits SOCS-1 function by targeting it for proteasomal degradation.

TRIM11

TRIM11 is a member of the protein family composed of a RING finger domain, which is a putative E3 ubiquitin ligase, a B-box domain, a coiled coil domain and a SPRY domain. A recent experiment with yeast two-hybrid screening has revealed that TRIM11 can interact with Humanin[91] which is a newly identified anti-apoptotic peptide that specifically suppresses Alzheimer's disease (AD)-related neurotoxicity. It is known that Bax

(Bcl2-associated X protein) has a crucial role in apoptosis. In response to death stimuli, Bax protein changes the conformation exposing membrane-targeting domains, translocates to mitochondrial membrane and releases the cytochrome c and other apoptogenic proteins. Indeed, Humanin is shown to bind with Bax and prevents the translocation of Bax from cytosol to mitochondria.[92] Moreover, Humanin blocks Bax association with isolated mitochondria and suppresses cytochrome c release. Therefore, Humanin seems to exert its anti-apoptotic effect by interfering the Bax function.

The coiled coil domain of TRIM11 is indispensable for the interaction with Humanin. The SPRY domain also contributes to the recognition of Humanin, whereas SPRY domain alone cannot. It was found that the intracellular level of Humanin was drastically reduced by the coexpression of TRIM11, and mutation of the RING finger domain or treatment with proteasome inhibitor attenuates the effect of TRIM11 on the intracellular level of Humanin.[91] These results suggest that the TRIM11 participates in the ubiquitin-mediated degradation of Humanin as an E3 ligase.

SSA/Ro (SSA1, TRIM21)

Sjögren syndrome is an autoimmune disease in which exocrine glands including salivary and lacrimal glands develop a chronic inflammation, and whose symptoms are dry eyes, dry mouth and fatigue. Autoantibodies to Ro recognize a ribonucleoprotein complex composed of small single-stranded RNAs and of one or more peptides. Although the Ro autoantigen is heterogeneous and found in most tissues and cells with differences in structure and quantity across tissues, it is detected in 35 to 50% of patients with systemic lupus erythematosus and in up to 97% of patients with Sjögren syndrome.[93] The 60-kD protein (Ro60) and the 52-kD protein (Ro52) were identified[94] and, another novel 56-kD protein (Ro56/SS-56) has been identified, recently.[95] Ro52 and Ro56 proteins belong to RBCC-SPRY subfamily. It is thought that the Ro autoantigen is involved in the regulation of transcription because it possesses functional domains associated with gene-regulation and binds to nucleic acids.[93] Its precise function is not understood, however. In a study, Ro52 was reported to be ubiquitinated in the cell.[96] The observation suggests that Ro52 may be downregulated by the ubiquitin–proteasome pathway in vivo. Interestingly, sera from patients with Sjögren syndrome showed heterogeneity in their reactivity to poly-ubiquitinated Ro52, probably because of their differing antigenic determinants. This heterogeneity of the reactivity may be associated with the varying clinical features found in Sjögren patients.

Conclusion

Here, we summarized the structural characteristics and functions of RING finger proteins specifically in terms of the E3 ligase activity. However, relatively few proteins have been really proven to function as E3 ligase. Thus, most RING finger proteins remain to be further investigated. Investigation of the RING finger proteins as a novel E3 ligase family will elucidate important mechanisms of cellular protein degradation and provide new insight into the physiological and pathophysiological roles of the pathway. Particularly, the molecular mechanisms of specific substrate recognition by E3 with the RING and other associated domains must be determined. Moreover, the RING finger proteins such as PML may possess unknown functions other than E3 ligase. Functional analysis of the RING finger proteins will help to understand biological roles of the family including the ubiquitin-mediated protein degradation pathway.

References

1. Freemont PS, Hanson IM, Trowsdale J. A novel cysteine-rich sequence motif. Cell 1991; 64(3):483-484.
2. Lovering R, Hanson IM, Borden KL et al. Identification and preliminary characterization of a protein motif related to the zinc finger. Proc Natl Acad Sci USA 1993; 90(6):2112-2116.
3. Borden KL, Boddy MN, Lally J et al. The solution structure of the RING finger domain from the acute promyelocytic leukaemia proto-oncoprotein PML. Embo J 1995; 14(7):1532-1541.
4. Barlow PN, Luisi B, Milner A et al. Structure of the C3HC4 domain by 1H-nuclear magnetic resonance spectroscopy. A new structural class of zinc-finger. J Mol Biol 1994; 237(2):201-211.
5. Bellon SF, Rodgers KK, Schatz DG et al. Crystal structure of the RAG1 dimerization domain reveals multiple zinc-binding motifs including a novel zinc binuclear cluster. Nat Struct Biol 1997; 4(7):586-591.
6. Gervais V, Busso D, Wasielewski E et al. Solution structure of the N-terminal domain of the human TFIIH MAT1 subunit: New insights into the RING finger family. J Biol Chem 2001; 276(10):7457-7464.
7. Zheng N, Wang P, Jeffrey PD et al. Structure of a c-Cbl-UbcH7 complex: RING domain function in ubiquitin-protein ligases. Cell 2000; 102(4):533-539.
8. Freemont PS. The RING finger. A novel protein sequence motif related to the zinc finger. Ann N Y Acad Sci 1993; 684:174-192.
9. Saurin AJ, Borden KL, Boddy MN et al. Does this have a familiar RING? Trends Biochem Sci 1996; 21(6):208-214.
10. Takeuchi M, Rothe M, Goeddel DV. Anatomy of TRAF2. Distinct domains for nuclear factor-kappaB activation and association with tumor necrosis factor signaling proteins. J Biol Chem 1996; 271(33):19935-19942.
11. Sato T, Irie S, Reed JC. A novel member of the TRAF family of putative signal transducing proteins binds to the cytosolic domain of CD40. FEBS Lett 1995; 358(2):113-118.
12. Cheng G, Cleary AM, Ye ZS et al. Involvement of CRAF1, a relative of TRAF, in CD40 signaling. Science 1995; 267(5203):1494-1498.
13. Rothe M, Sarma V, Dixit VM et al. TRAF2-mediated activation of NF-kappa B by TNF receptor 2 and CD40. Science 1995; 269(5229):1424-1427.
14. Takahashi R, Deveraux Q, Tamm I et al. A single BIR domain of XIAP sufficient for inhibiting caspases. J Biol Chem 1998; 273(14):7787-7790.
15. Liston P, Fong WG, Kelly NL et al. Identification of XAF1 as an antagonist of XIAP anti-Caspase activity. Nat Cell Biol 2001; 3(2):128-133.
16. Yang Y, Fang S, Jensen JP et al. Ubiquitin protein ligase activity of IAPs and their degradation in proteasomes in response to apoptotic stimuli. Science 2000; 288(5467):874-877.
17. Clem RJ, Miller LK. Control of programmed cell death by the baculovirus genes p35 and iap. Mol Cell Biol 1994; 14(8):5212-5222.
18. van der Reijden BA, Erpelinck-Verschueren CA, Lowenberg B et al. TRIADs: A new class of proteins with a novel cysteine-rich signature. Protein Sci 1999; 8(7):1557-1561.
19. Kitada T, Asakawa S, Hattori N et al. Mutations in the parkin gene cause autosomal recessive juvenile parkinsonism. Nature 1998; 392(6676):605-608.
20. Morett E, Bork P. A novel transactivation domain in parkin. Trends Biochem Sci 1999; 24(6):229-231.
21. Imai Y, Soda M, Inoue H et al. An unfolded putative transmembrane polypeptide, which can lead to endoplasmic reticulum stress, is a substrate of Parkin. Cell 2001; 105(7):891-902.
22. Imai Y, Soda M, Hatakeyama S et al. CHIP is associated with Parkin, a gene responsible for familial Parkinson's disease, and enhances its ubiquitin ligase activity. Mol Cell 2002; 10(1):55-67.